

MECHANISMS OF CAVITATION DAMAGE STUDIES USING SOFT ALUMINIUM

SOBEIH M.A. SELIM*

ABSTRACT

A study has been made of the mechanisms of cavitation damage in a soft aluminium using a vibratory system. A series of stationary specimens of soft aluminium were subjected to the cavitation produced by the vibratory in water. The resulting surface deformation was analysed using a surface roughness measuring device. Moreover, photographs of the eroding surface has been presented.

By virtue of the features of the pits formed, it is concluded that while there are several contributory mechanisms, the most intense damage was caused by the impingement of high velocity microjets on the material surface during bubble collapse.

1. INTRODUCTION

Although the effects of cavitation have been observed long ago, the actual mechanics of bubble collapse was not observed due to the high velocities involved. The mechanisms by which the erosion of a material occurs during cavity collapse are of fundamental importance to the study of cavitation erosion because the formulation of a theoretical treatment of

* Lecturer, Department of Mechanical Power Engineering,
Faculty of Engineering & Technology, Menoufia University,
Shiben El-Kom, Egypt.

cavitation erosion depends upon the damage mechanism. Cavitation researches have shown that the damage mechanism caused by the bubble collapse could be explained by one of two theories, which are the mechanical and the chemical. The mechanical theory asserted that the damage was done to the eroding surface by impingement of shock waves produced by collapsing bubbles. The chemical theory postulated erosion caused by electric discharges. Most investigators agreed that the cavitation erosion is primarily due to mechanical attack with additional effects due to interaction between mechanical and chemical aspects of the problem.

The rate of material removal due to chemical attack appears insignificant compared with the mechanical attack. Even if the cavitation damage is the result of totally mechanical attack, there are still a number of mechanical mechanisms that are possible. The possible mechanical mechanisms that have proposed to explain cavitation damage are :

- [1] Pressure wave model. This assumed that bubble collapse was spherically symmetric, which when arrested resulted in the propagation of a spherical pressure wave being imposed on any material surface close to the centre of bubble collapse.
- [2] Microject model. This postulated that during the non-spherical collapse a high velocity microject was produced which impinged on any material surface close to the centre of the bubble collapse.

Until a few decades ago, the first mechanism which was proposed by Rayleigh [1], was accepted as the more realistic explanation for the erosion of materials. Rayleigh's analysis has been improved by several investigators. It was found that the pressure can reach

extremely high values ($10^2 - 10^4$ MN/m² at an ambient pressure of 0.1 MN/m² and with cavity gas pressure 10^{-4} MN/m²). The shock wave intensity decreases inversely proportional to the radius from the centre, and close to this it would certainly be able to damage surfaces of solids.

Kornfeld and Suvorov [2] suggested that liquid jets could be formed during cavity collapse. Eisenberg [3] speculated that jets formed during the asymmetrical collapse of cavitation bubbles could be responsible for the damage. These jets were experimentally shown by Naude and Ellis [4]. The occurrence of jet formation during collapse of single cavities was supported photographically by Kling and Hammitt [5], Lauterborn [6], Brunton [7] and Popoviciu [8]. The collapse of an initially spherical cavity near to a solid wall was determined theoretically by Plesset and Chapman [9]. The jet velocity was found to be 130 m/s at a collapse pressure of 0.1 Mn/m². This implies an impact pressure up to 200 MN/m² when the jet strikes the solid wall. This impact pressure is sufficient to cause the observed cavitation damage in strong materials.

It is the object of the present paper to select one of these mechanisms of erosion from the other.

2. EXPERIMENTAL APPARATUS AND SPECIMENS

The experimental apparatus used is a vibratory in which frequency and amplitude of vibration can be adjusted. Fig.1 illustrates diagrammatically the experimental arrangement. The vibratory was driven by a 500 Watts variable speed universal motor. The face diameter of the vibratory end was 25 mm and the normal peak-to-peak amplitude was approximately 0.25 mm. The

pressure wave generated resulted in the formation of cavitation bubble in the gap between the stationary specimen face and the end of the vibratory. The gap between the end of the vibratory and the specimen face was adjusted using feeler gauges. Specimens exposed to cavitation were placed in a specimen holder which itself fixed to the apparatus frame. The Specimen holder has a circular hole for mounting of 23 mm specimen with the specimen surface flush with the surface of the holder.

The specimens used for the present experiments were turned from a soft aluminium rod. The specimens were polished to obtain a smooth specimen surface. The specimens were examined by optical microscope before being exposed to cavitation to determine qualitatively when the polishing process was finished. The specimen and the vibratory end were immersed in a beaker containing approximately 1 litre of tap water at 34°C. The temperature of water was checked from time to time during the tests, and the variation was found to be negligible.

The erosion specimens were analysed using a FÖRSTER profilograph Model 5815 at Faculty of Engineering and Technology, Helwan University. The scanning device used to measure the surface profiles has a diamond stylus with a rounded tip about 10 μm . The stylus speed across the specimen surface and the operative length of traverse were kept the same for all the tests. This was accomplished by setting the operative length of traverse equal to 10 mm and the speed equal to 0.5 mm/s. Photographs of erosion specimens were taken using optical metallurgical microscopes which is provided with a camera.

3. EXPERIMENTAL RESULTS AND DISCUSSION

The experiments were performed at 480 C/S and a double amplitude of 0.25 mm. Visual observations using stroboscopic light through a glass beaker show that the bubble field between the vibratory and specimen surface consist of a cloud of mainly small bubbles.

All specimens exposed to cavitation have been studied by optical microscope. These investigations reveal that right from the beginning of cavitation exposure plastically deformed areas occur on the originally smooth surface. During the first part of the cavitation exposure the deformed areas are clearly separated indicating that each of them is caused by the collapse of a single cavity. If specimens are exposed to cavitation for different times but at a fixed cavitation condition, the maximum number of dents per mm^2 is expected to increase proportional to exposure time. This is verified by counting the number of dents in small square (2 x 2 mm) over the central area of the eroded specimen during the first part of the exposure time. The same trend was reported by Knapp [10], Hanson and Mørch [11] and Lobo Guerrero [12]. At further cavitation exposure the dents are found to start overlapping, and a highly distorted surface develops with deformations of larger scale. The density of pits reaches a maximum when overlapping becomes significant and a further cavitation exposure the density of dents falls to a somewhat lower but constant level. This is shown in Fig. 2, which covers exposure time up to 300 sec. The reason that the dents density reaches a maximum and then becomes constant is due to the interface of the damage areas and transformation of the overlapping dents into one large crater

by a new cavity collapse in between them as shown in Figs 3 and 4.

During the counting procedure the distribution of dent sizes on the specimen surface were measured for each dent. Fig.5 shows the size distribution of the dents. This figure indicates that the percentage of dents of a given size always increases as the size under consideration is decreased, reaching a peak and thereafter decreasing. The range of dent sizes was found to be approximately 0.1-0.4 mm and over 50% of all dents were in the smallest sizes. Hammitt [13] has suggested that the diameter of typical microjets resulting from cavitation bubble collapse was in the range 1-80 μm , which is smaller than the dent size observed in the present experiments. The reason for this difference is that during the impact of the jet with the surface and during the formation of dent itself an outward flow of the liquid occurs resulting in a dent size larger than the microjet diameter. However, the present experiments are not sufficient to give conclusive proof about the microjet size from the size of dents formed. Nevertheless, these values of dent sizes (0.1-0.4 mm) are compatible with the dent diameter observed with Knapp [10] using annealed aluminium. Dent diameters of 0.25 mm observed by Brunton [7] using thin metal foil.

Figs 7-11 are photographs and surface measurements of deformed areas at different exposure times. Fig.6 is a photograph of the specimen surface before being exposed to cavitation. This is to allow a visual comparison to be made between the eroded and virgin surfaces. Figs 12-16 are photographic enlargements of

erosion areas seen in Figs. 7-11, respectively. In general these figures show that the form of erosion pattern is deep dents in the central area of specimen. Figs. 12-16 show that the rim associated with the dents is not symmetrical. For this case, spherical collapse was unlikely because of the irregularity of the dents and the microjet mode is the cause of damage. Moreover, figures 9-11 (surface measurements) indicate that the performance of the bottom of dents is suggestive of jetting. This is because a shock wave in a depression would favour rounded hemispherical craters while repeated jetting leads to conical elongated pits as shown in Figures 9-11. Smaller and shallower depressions appearing in large numbers are probable formed by microjets which are less intense than those necessary to form deep holes, if these are formed by a single cavitation event. Assuming that the damage is caused by microjets it is clear from the photographs and surface measurements that the collapse of cavitation bubbles results in a wide range of microjet intensities as described by their diameters.

4. CONCLUSIONS

The conclusions which can be drawn from these studies are :

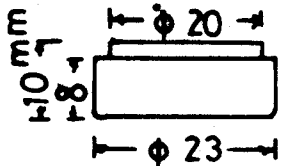
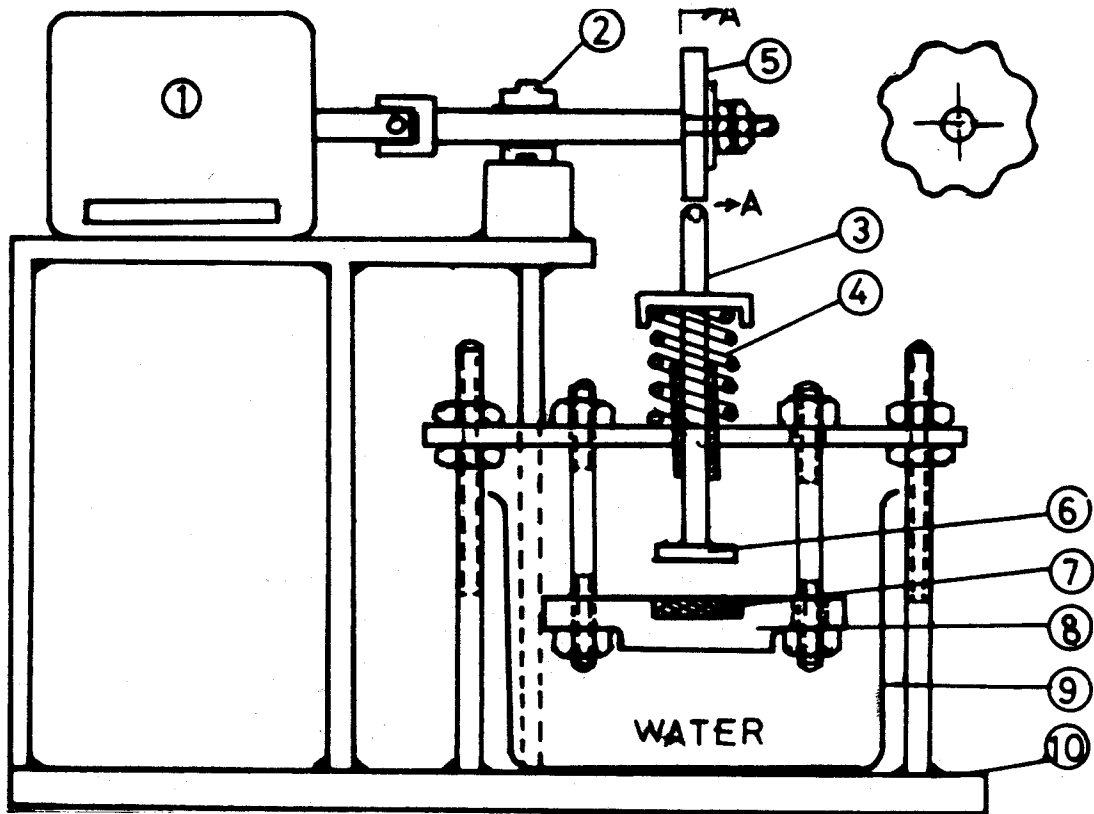
- 1] No evidence of surface damage was found which could be linked directly with the spherical pressure wave mechanism.
- 2] The photographic evidence included in this paper does strongly indicate that microjets are the dominant cause of damage.
- 3] Using a vibratory device to produce cavitation, a wide range of microjet intensities result from the collapse of cavitation bubbles generating by the acoustic pressure field.

- 4] In the light of the present results, the formulation of a theoretical model for bubble collapse to produce scaling laws can be obtained.

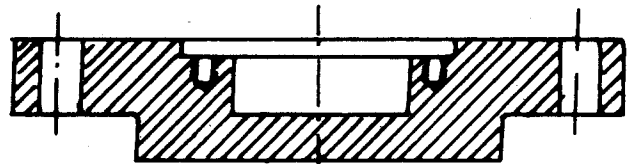
REFERENCES

- 1] Rayleigh, Lord, "On the Pressure Developed in a Liquid During the Collapse of a Spherical Cavity", Phil. Mag, (1917), 34, 94.
- 2] Kornfield, M. and Suvorov, L., "On the Destructive Action of Cavitation", J. Applied Physics. Vol 15, (1944), pp 495-506.
- 3] Eisenberg, P., "On the Mechanism and Prevention of Cavitation", David Taylor Model Basin Report 712, Washington, D.C., (1950).
- 4] Naude, C.F. and Ellis, A.T., "On Mechanism of Cavitation Damage by Non-Hemispherical Cavities collapsing in contact with a Solid Boundary", Trans. ASME, J. Basic Engr., 83, D, 4, (1961).
- 5] Kling, C.L. and Hammitt, F.G., "A photographic study of Spark Induced Cavitation Bubble Collapse", Trans. ASME, J. Basic Engr, 94, D, 4, (1972).
- 6] Lauterborn, W., "Liquid jet from Cavitation Bubble Collapse", Proc. 5th inter. Conf. on Erosion by Solid and Liquid Impact, Cambridge, England, Sept. (1979).
- 7] Brunton, J.A., "Cavitation Damage", Proc. 3rd Int. Conf. on Rain Erosion, Royal Aircraft Establishment, Farnborough, U.K. (1970).
- 8] Popoviciu, M., "A photographic Study of Spherical Bubbles Dynamics", Proc. of 4th Conf. on Fluid Machinery, Budapest, (1972).

- 9] Plesset, M.S. and Chapman, R.B. "Collapse of an Initially Spherical Vapour Cavity in the Neighbourhood of a Solid Boundary", J. Fluid Mech., Vol. 47, (1971).
- 10] Knapp, R.T., "Recent Investigation of the Mechanics of Cavitation and Cavitation Damage", Trans. ASME, Oct. (1955).
- 11] Hansson, I. and Morch, K.A., "The Initial stage of Cavitation Erosion on Aluminium in Water Flow", J. Phys. D. : Appl. phys, Vol. 11, (1978).
- 12] Lobo Guerrero, J., "A Study of the Damage Capacity of Some Cavitating Flows", Ph. D. Thesis, Southampton University, (1974).
- 13] Hammitt, F.G., "Cavitation and Multiphase Flow Phenomena", McGraw-Hill Co. New York. (1980).



⑦ SPECIMEN



⑧ SPECIMEN HOLDER

- ① Electric motor
- ② Bearing
- ③ Vibratory
- ④ Spring
- ⑤ Can

- ⑥ Vibratory end
- ⑦ Specimen
- ⑧ Specimen holder
- ⑨ Beaker
- ⑩ Frame

Fig.1. Diagrammatic arrangement of experimental vibratory apparatus.

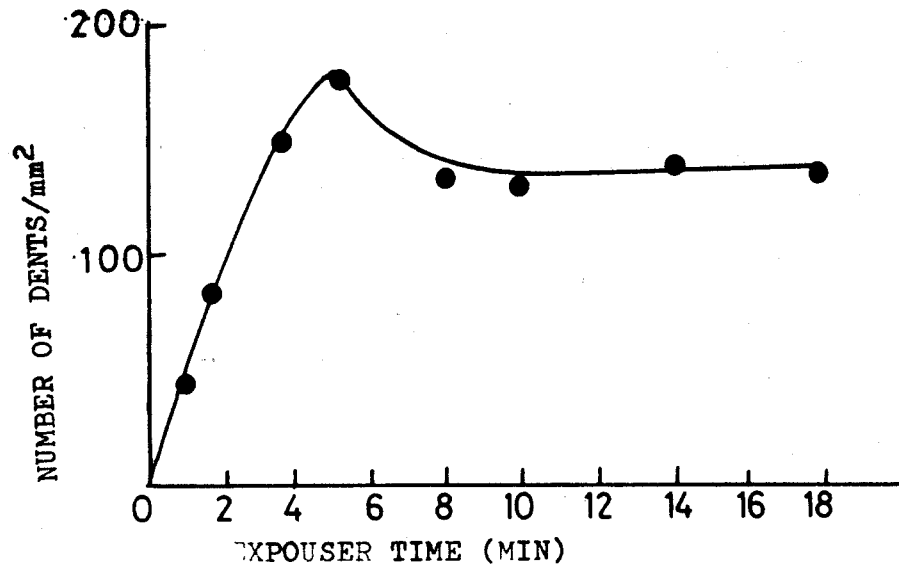


Fig.2. Density of dents against cavitation time.



Fig.3.

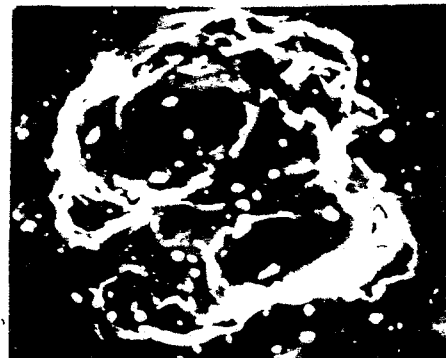


Fig.4.

Figs. 3 and 4. Overlapping many dents to form large craters(x100)

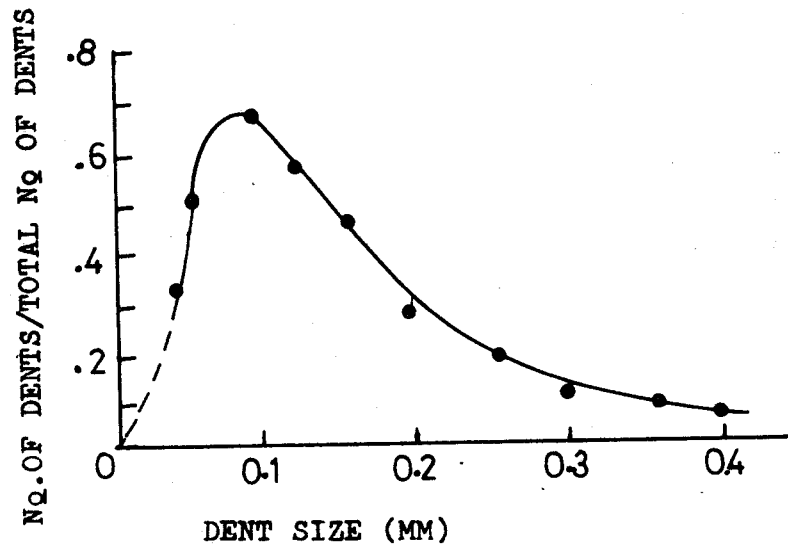


Fig. 5. Size distribution.

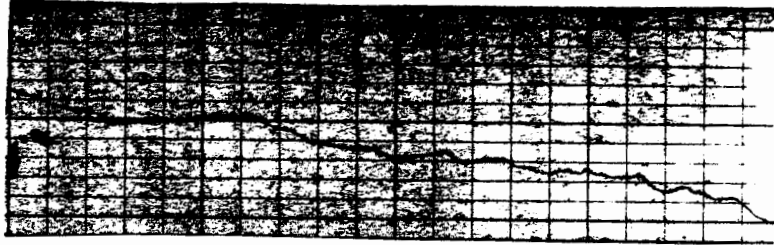
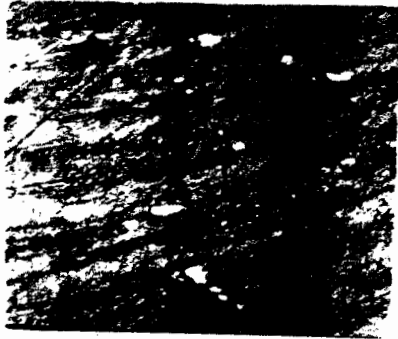


Fig. 6. Photograph and surface profile of aluminium before exposure to cavitation.

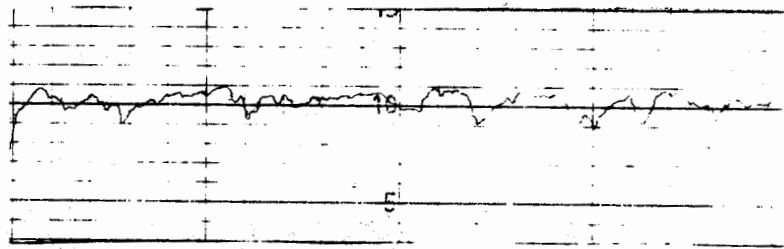


Fig. 7. Exposure time 50 sec.

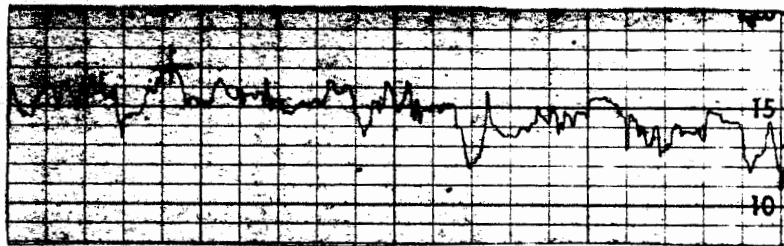


Fig.8. Exposure time 110 sec.

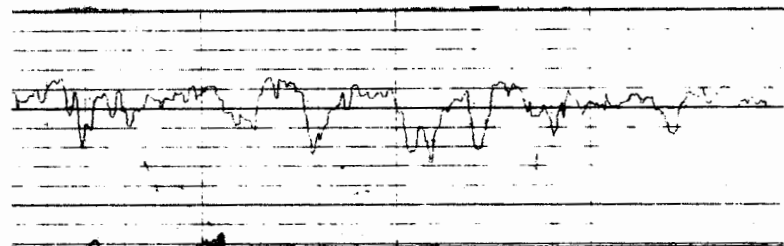
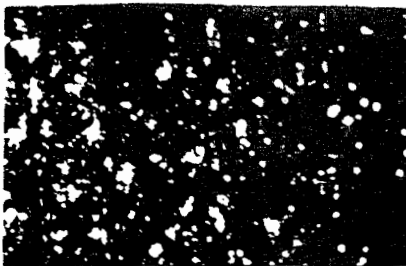


Fig.9. Exposure time 4 min.

Figs.7-9. Photographes and surface measurements of maximum deformed areas at different exposure time(x5).

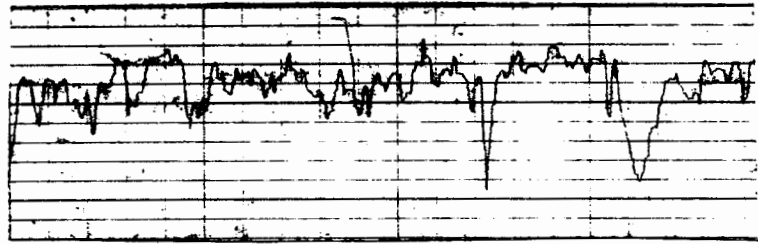


Fig.10. Exposure time 7 min.

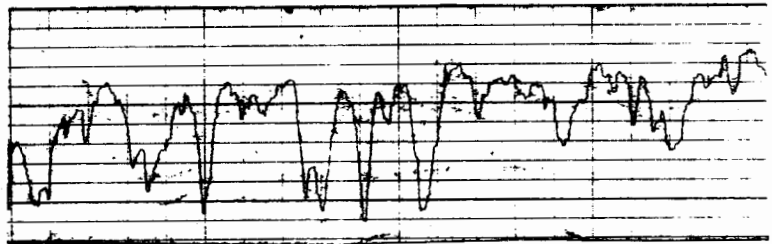
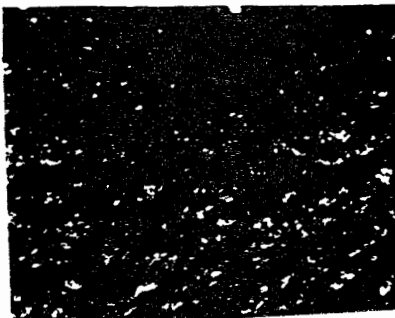


Fig.11. Exposure time 11 min.

Fig.10 and 11. Potographs and surface roughness measurements of aluminium after exposure to cavitation (x5).



Fig.12.



Fig. 13.



Fig.14.



Fig.15.

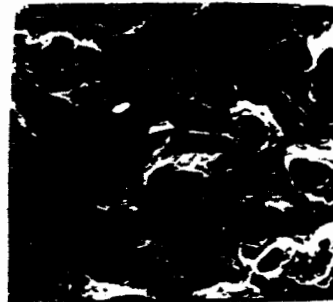


Fig.16.

Figs.12 to 16. Photographic enlargements of erosion areas in figures 7 to 11 respectively (x25).